WVT-TR-76033

APPROXIMATE ANALYSIS OF THE INITIAL PRESSURE DISTRIBUTION WITHIN A 105MM MUZZLE BRAKE

H. J. Sneck

August 1976

BENET WEAPONS LABORATORY
WATERVLIET ARSENAL
WATERVLIET, N.Y. 12189

TECHNICAL REPORT

AMCMS No. 662603.11.H7800

DA Project No. 1W662603AH78

DISCLAIMER

The findings in this report are not to be construed as an official Department of the Army position unless so designated by other authorized documents.

The use of trade name(s) and/or manufacturer(s) in this report does not constitute an official indorsement or approval.

DISPOSITION

Destroy this report when it is no longer needed. Do not return it to the originator.

SECURITY CLASSIFICATION OF THIS PAGE *(When Data Entered)*

REPORT DOCUMENTATION PAGE

READ INSTRUCTIONS BEFORE COMPLETING FORM

1. REPORT NUMBER: WVT-TR-76	2. GOVT ACCESSION NO.
3. RECIPIENT'S CATALOG NUMBER	
4. TITLE *(and Subtitle)*: Approximate Analysis of the Initial Internal Pressure Distribution within a 105mm Muzzle Brake	5. TYPE OF REPORT & PERIOD COVERED
	6. PERFORMING ORG. REPORT NUMBER
7. AUTHOR(s): H. J. Sneck	8. CONTRACT OR GRANT NUMBER(s)
9. PERFORMING ORGANIZATION NAME AND ADDRESS: Benet Weapons Laboratory Watervliet Arsenal, Watervliet, NY 12189 SARWV-RT-TP	10. PROGRAM ELEMENT, PROJECT, TASK AREA & WORK UNIT NUMBERS AMCMS No. 662603.11.H7800 DA PROJ No. 1W662603AH78
11. CONTROLLING OFFICE NAME AND ADDRESS: US Army Armament Command Rock Island, IL 61201	12. REPORT DATE: August 1976
	13. NUMBER OF PAGES: 29
14. MONITORING AGENCY NAME & ADDRESS *(if different from Controlling Office)*	15. SECURITY CLASS. *(of this report)*: Unclassified
	15a. DECLASSIFICATION/DOWNGRADING SCHEDULE

16. DISTRIBUTION STATEMENT *(of this Report)*

Approved for public release; distribution unlimited

17. DISTRIBUTION STATEMENT *(of the abstract entered in Block 20, if different from Report)*

18. SUPPLEMENTARY NOTES

19. KEY WORDS *(Continue on reverse side if necessary and identify by block number)*

Muzzle Brakes
Muzzle Pressure
Method of Characteristics
Supersonic Flow

20. ABSTRACT *(Continue on reverse side if necessary and identify by block number)*

The method of characteristics is used to predict propellent gas pressure on an experimental muzzle brake attached to a 105mm M68 gun. The analysis is limited to the time during which the gas reaches and impinges on the baffles.

The purpose of the analysis was to develop a means of predicting pressure distributions for use in stress analyses of muzzle brakes.

DD FORM 1 JAN 73 1473 EDITION OF 1 NOV 65 IS OBSOLETE

SECURITY CLASSIFICATION OF THIS PAGE *(When Data Entered)*

TABLE OF CONTENTS

LIST OF FIGURES

INTRODUCTION

This analysis will attempt to predict propellent pressures which act on various parts of a muzzle brake. These pressures will then serve as inputs to a stress analysis of the brake. The 105mm M68 gun and an experimental howitzer brake, fitted to the gun, were selected because the gun is being fired in a life test. For economy, pressures on the brake will be measured during a few of those rounds to check the analysis.

The internal pressures created in approximately the first 66 microseconds following the barrel uncorking are analyzed. The analysis is broken into two parts, one for the diffuser section of the brake, and one for the downstream portion through which the gases exhaust to the atmosphere. Both flows are modeled as one-dimensional during the short period of time which it takes for the uncorked gases to reach the end of the brake.

No attempt is made to predict the flow fields or the pressures produced by it at subsequent times, although approximate methods might be developed to do so, should the predictions of this analysis yield results in reasonable agreement with experiment.

ANALYSIS OF BLOW-BY

At the instant that the projectile uncorks the barrel a shock wave is formed in the brake at the muzzle. This shock wave propagates down the diverging annular space between the projectile and the inside wall of the muzzle brake. The flow initiated by this shock wave represents a leakage of high pressure gas from behind the projectile. (See Figure 1).

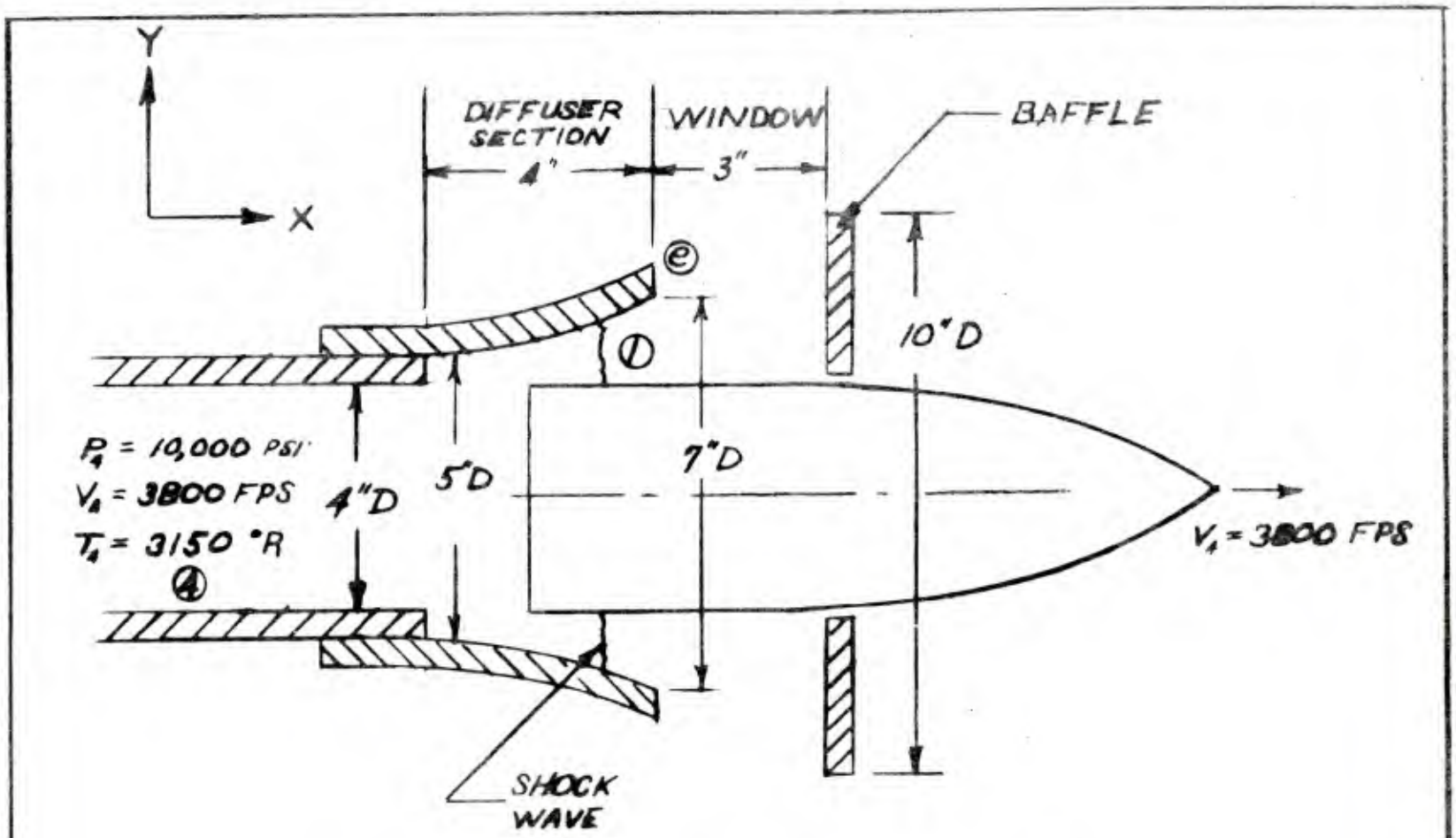

Figure 1. Projectile and brake at muzzle uncorking.

Figure 2 shows the various regions associated with the sudden release of high pressure gas into the annulus following the uncorking. The gas which escapes through this annulus traverses an area change with a ratio

(1) $$\frac{A_1}{A_4} = \frac{(5)^2-(4)^2}{(4)^2} = \frac{9}{16}$$

The equivalent diameter ratio for this area change is

(2) $$\frac{D_1}{D_4} = \sqrt{\frac{A_1}{A_4}} = \frac{3}{4}$$

According to Alpher and White[1] the effect of an area change in a shock tube can be accounted for by introducing a factor (g) into the standard shock tube "burst" equation so that it takes the modified form

(3) $$\frac{P_4}{P_1} = \frac{\frac{1}{g}\left[\frac{2\gamma_1 M_s^2 - (\gamma_1-1)}{\gamma_1+1}\right]}{\left[1-\left(\frac{\gamma_4-1}{\gamma_1+1}\right)\frac{C_1}{C_4}\left(M_s-\frac{1}{M_s}\right)\left(\frac{1}{g}\right)+\left(\frac{\gamma_4-1}{2}\right)\frac{V_4}{C_4}\right]^{\frac{2\gamma_4}{\gamma_4-1}}}$$

In this equation subscripts refer to the regions so numbered in Fig 2 and:

T_1 = 530°R

T_4 = 3150°R

γ_1 = 1.4 (air)

γ_4 = 1.25 (combustion products)

1. R. A. Alpher and D. R. White, "Ideal Theory of Shock Tubes with Area Change Near the Diaphragm" G. E. Rpt 57-RL-1664, Jan 1957

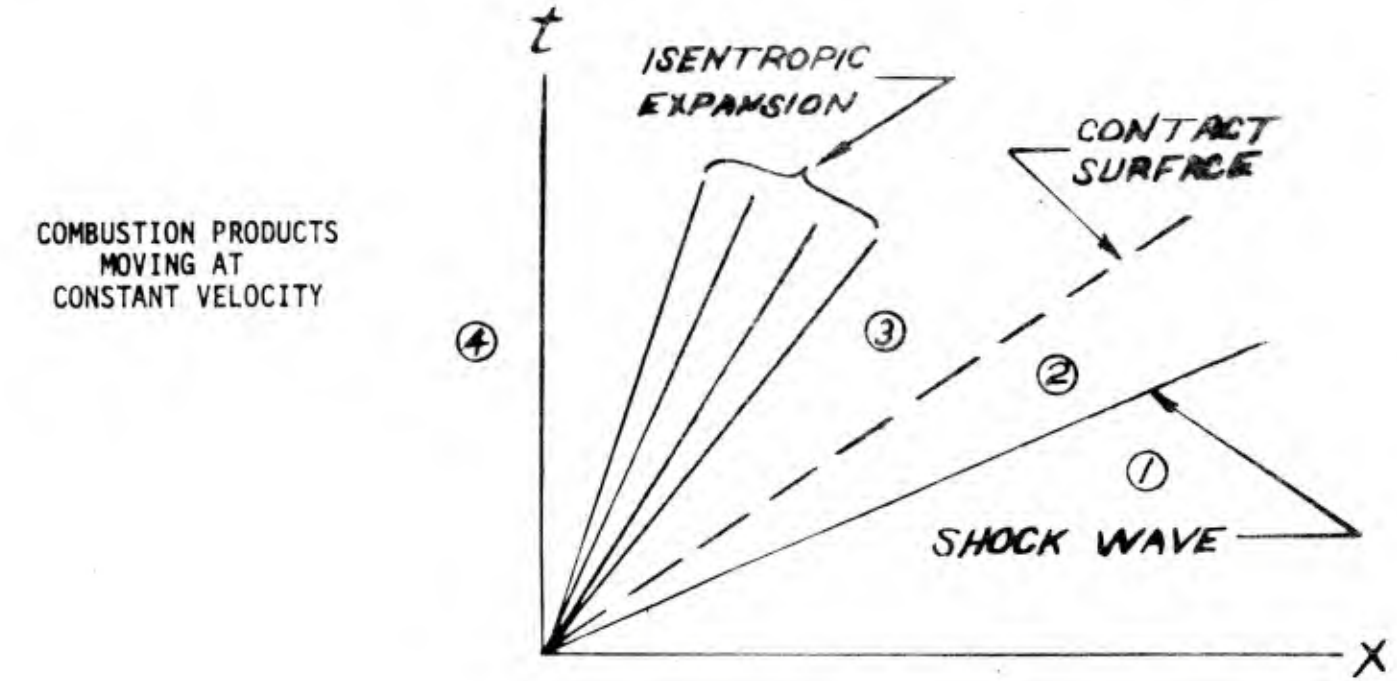

Figure 2. Wave diagram for annular leakage at uncorking.

V_4 = 3800 ft/sec (projectile velocity)

g = 1.25 for D_4/D_1 = 4/3

R_1 = 53.3 ft-lbf/lbm °R (air)

R_4 = 67.0 ft-lbf/lbm °R (combustion products)

ρ_4 = 6.82 lbm/ft^3

g_c = gravitational constant = 32.2 lbm ft/lbf sec^2

$C_4 = \sqrt{\gamma_4 g_c R_4 T_4}$ = 2918 ft/sec

P_4/P_1 = 10,000/15 = 667

$\frac{C_1}{C_4} = \sqrt{\frac{1.4\ (53.3)\ 530}{1.25\ (67)\ 3150}}$ = 3.86

With these inputs, equation (3) becomes

(3a)

$$667 = \frac{0.933M_s^2 - 0.133}{\left[1.163-0.0393(M_s-1/M_s)\right]^{10}}$$

Solving this equation (3a) for the initial shock Mach number (M_s) yields a value of 9.2. The shock wave itself travels with a velocity of 9.2 (1130) = 10,396 ft/sec while the fluid which it sets into motion moves with a velocity given by

(4)

$$v_2 = \frac{2}{\gamma_1+1} C_1 \left(M_s - \frac{1}{M_s}\right)$$

$$= \frac{2}{2.4} (1130) \left(9.2 - \frac{1}{9.2}\right)$$

$$v_2 = 85.61 \text{ ft/sec}$$

Obviously the shock wave and the fluid behind are traveling much faster than the projectile, reaching the end of the diffuser section of the brake (4" from the muzzle) before the base of the projectile does.

The propagation of a shock wave through an area change has been investigated by Whitman[2] who showed that

(5) $$M_e = Ms \left(\frac{As}{Ae}\right)^{\frac{K\infty}{2}} \quad \text{where } K_\infty = .36$$

$$\approx 9.2 \left[\frac{(5)^2 - (4)^2}{(7)^2 - (4)^2}\right]^{0.18}$$

$$M_e = 7.28$$

The conditions behind the shock wave at the exit of the diffuser are given by

(6) $$\frac{P_e}{P_1} = \frac{2\gamma_1}{\gamma_1+1} M_e^2 - \frac{\gamma_1-1}{\gamma_1+1}$$

$$= \frac{2.8}{2.4} (7.28)^2 - \frac{0.4}{2.4}$$

$$\frac{P_e}{P_1} = 61.7$$

(7) $$\frac{\rho_e}{\rho_1} = \frac{(\gamma_1+1) M_e^2}{(\gamma_1-1) M_e^2 + 2}$$

$$\frac{\rho_e}{\rho_1} = 5.48$$

(8) $$T_e = \frac{P_e \rho_1}{P_1 \rho_e} T_1$$

$$T_e = \frac{(61.7)}{(5.48)} 530 = 5964°R$$

2. G. B. Whitman, "On the Propagation of Shock Waves through Regions of Non-Uniform Area Flow," J. Fluid Mechanics, Vol. 2, P. 337 (1958)

(9) $$v_e = \left(\frac{2}{\gamma_1+1}\right) c_1 \left(M_e - \frac{1}{M_e}\right)$$

$$v_e = 6726 \text{ ft/sec}$$

The leakage passed by the projectile (blow-by) can be estimated from

(10) $$\dot{m} = \rho_e A v_e$$

$$= \frac{5.48(0.075)}{144} \left(\frac{49-16}{4}\right) (6726) \pi$$

$$\dot{m} = 497.6 \text{ lbm/sec}$$

The time for the projectile base to reach the end of the diffuser is $\frac{x}{\dot{x}} = \frac{4/12}{3800} = 8.77\ (10^{-5})$ sec so that the total leakage during this period is 0.0436 lbm which is only a few percent of the total mass and therefore quite negligible.

ANALYSIS OF THE GAS FLOW BEHIND THE PROJECTILE

Since very little of the barrel gas is lost via blow-by as the projectile base moves through the diffuser section, most of the gas which was behind the projectile base at uncorking must still be behind the base when it reaches the diffuser exit (e).

If it is assumed that this gas undergoes an isentropic expansion, then the pressure at this point must be approximately

(11) $$\frac{P_{41}}{P_4} = \left(\frac{V_4}{V_{41}}\right)^{\gamma_4}$$

Therefore $$P_4{}^1 = 10{,}000 \left(\frac{16}{49}\right)^{1.25}$$

$$P_4{}^1 = 2468 \text{ psia}$$

(12) $$T_{41} = T_4 \left(\left(\frac{P_4{}^1}{P_4}\right)\right)^{\frac{\gamma_4-1}{\gamma_4}}$$

$$T_{41} = 3150 \left(\left(\frac{2468}{10{,}000}\right)\right)^{\frac{0.25}{1.25}} \qquad T_{41} = 2381°R$$

(13) $$C_{41} = \sqrt{32.2\, R_{41} T_{41} \gamma_4}$$

$$C_{41} = \sqrt{1.25(32.2)67(2381)}$$

$$C_{41} = 2534 \text{ ft/sec}$$

(14) $$\rho_{41} = \rho_4 \frac{V_4}{V_{41}}$$

$$\rho_{41} = 6.82 \left(\frac{16}{49}\right) = 2.23 \text{ lbm/ft}^3$$

ANALYSIS OF DIFFUSER UNCORKING

Figure 3 illustrates the situation assumed to exist at the instant that the projectile base reaches the end of the diffuser. It will be assumed that the disk of fluid shown at the left of this figure propagates to the right with the projectile velocity $\dot{x}$, (3800 ft/sec) while expanding radially behind a radial shock wave. This assumption is analogous to that used in the report by Soifer[3] with the exception that the explosion does not emanate from a line source and is one-dimensional rather than cylindrical. The assumption of one-dimensional flow seems more realistic considering the presence of the brake side plates beyond the diffuser section. The burst of a finite size volume assumed here avoids the rather unrealistically low densities in the core of the burst which result from the assumption of a line source.

The shock Mach number for a shock wave propagating radially from the "window" of the muzzle brake is given by the equation

3. "Muzzle Brake Analysis," S & D Dynamics, Inc, TR # 73-6, Oct 73, Contr. No. DAAF 07-73-0541

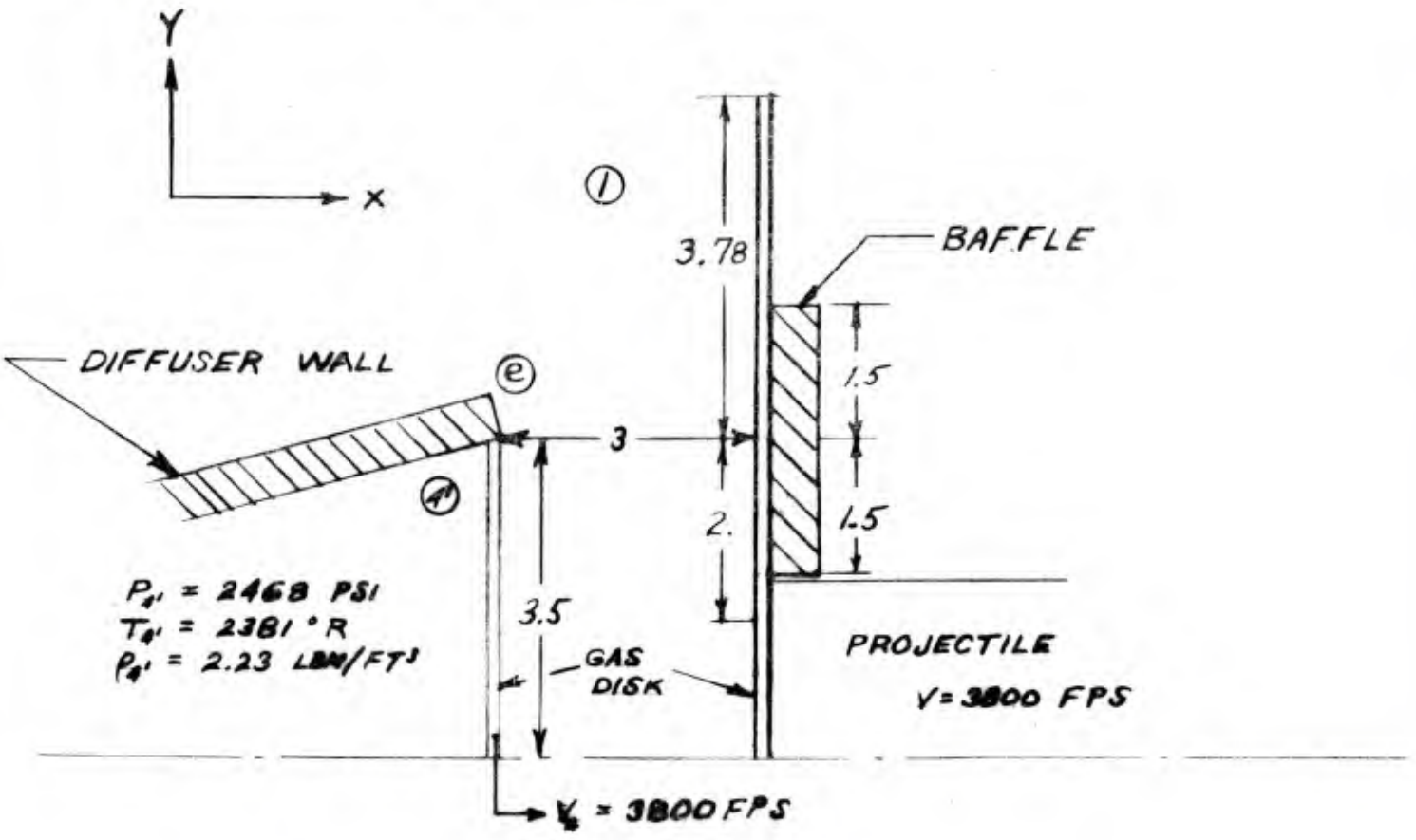

Figure 3. Shock wave propagation through the brake window.

(15) $$\frac{P_4'}{P_1} = \frac{\frac{2\gamma_1 M_S^2 - (\gamma_1 - 1)}{\gamma_1 + 1}}{\left[1 - \left(\frac{\gamma_4' - 1}{\gamma_1 + 1}\right)\frac{C_1}{C_4'}\left(M_S - \frac{1}{M_S}\right)\right]^{\frac{2\gamma_4'}{\gamma_4' - 1}}}$$

(15a) $$\frac{2468}{15} = \frac{1.167 M_S^2 - 0.167}{\left[1 - .0464\left(M_S - \frac{1}{M_S}\right)\right]^{7/0}} = 164$$

This equation is the same as equation (3) without the factor (g). Furthermore, the last term in the denominator of (3) vanishes here because v_{41}, the radial velocity, is initially zero in this radially expanding shock.

The shock Mach number for this one-dimensional shock wave moving at a right angle to the flight path is $M_S = 4.25$. Behind this shock wave

(16) $$v_{21} = \frac{2}{\gamma_1 + 1} C_1 \left(M_S - \frac{1}{M_S}\right) = 3774 \text{ ft/sec}$$

(17) $$\frac{\rho_{21}}{\rho_1} = \frac{(\gamma_1 + 1) M_S^2}{(\gamma_1 - 1) M_S^2 + 2} = 5.40$$

(18) $$\frac{P_{21}}{P_1} = \frac{2\gamma_1 M_S^2}{\gamma_1 + 1} - \left(\frac{\gamma_1 - 1}{\gamma_1 + 1}\right) = 20.9$$

(19) $$T_{21} = \frac{P_{21}}{P_1}\frac{\rho_1}{\rho_{21}} T_1 = 2051°R$$

The time required for the projectile base to move from the end of the diffuser to the baffle is $\frac{x}{\dot{x}} = \frac{3/12}{3800} = 6.58\ (10^{-5})$ sec.

During this time the leading edge of the radial shock wave travels a distance

(20) $$\Delta R = C_1 M_S \frac{x}{\dot{x}}$$

$$\Delta R = \frac{(C_1 M_S)}{(3800)} 3 = 3.78 \text{ in}$$

as shown in Figure 3. The trailing edge of the centered expansion fan travels a distance

(21) $$\Delta r = C_{41} \frac{x}{\dot{x}} = C_{41}\, t$$

$$\Delta r = \left(\frac{2534}{3800}\right) 3 = 2.00 \text{ in}$$

Figure 4 shows the relative position of the characteristics and the shock front with respect to the baffle when the moving disk of gas impinges on it.

In order to find the pressure distribution on the baffle, the "backward" running characteristics (shown as a fan in Figure 4) are used to establish the location on the baffle while the forward running characteristics are used to carry the core conditions through the fan.

For example, the characteristic which intercepts the outer edge of the baffle has a slope of $\frac{1.5/12}{6.58(10^{-5})} = 1900$ ft/sec

therefore, the slope is equal to $U_o - C_o = 1900$ where the subscript o refers to the outer edge of the end plate. Since along the "forward" running characteristic (not shown in Figure 4), the value $u + \frac{2}{\gamma_4 - 1} c$ = constant = $8C_{41}$, i.e.,

(23) $$U_o + 8\, C_o = 8\, C_{41} = 8\,(2534)$$

Combining these two equations yields

$C_o = 2041$ ft/sec

$U_o = 3941$ ft/sec and

from (13) $$T_o = \frac{C_o^2}{32.2\,\gamma R}$$

$$T_o = \frac{(2041)^2}{(1.25)(67)(32.2)} = 1544\ ^\circ R$$

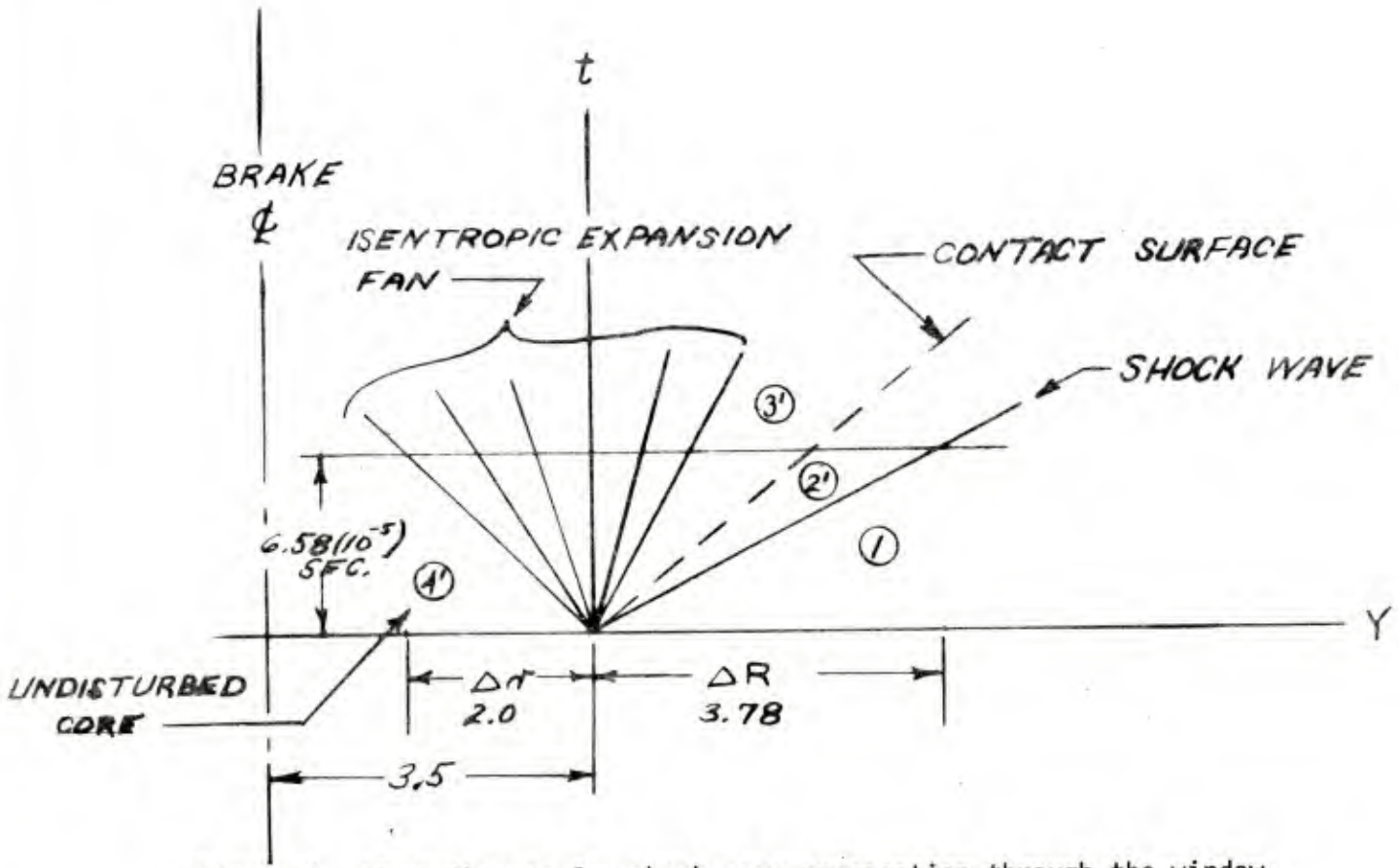

Figure 4. Wave diagram for shock wave propagation through the window.

from (12)

$$P_o = P_{4'}\left(\frac{T_o}{T_{4'}}\right)^{\frac{\gamma}{\gamma-1}}$$

$$P_o = 2468\left(\frac{1544}{2381}\right)^5 = 283 \text{ Psia}$$

(24)

$$\rho_o = \rho_{4'}\left(\frac{P_o}{P_{4'}}\right)^{\frac{1}{\gamma}}$$

$$\rho_o = 2.23\left(\frac{283}{2468}\right)^{0.8} = 0.394 \ \frac{\text{lbm}}{\text{Ft}^3}$$

The stagnation pressure rise due to momentum exchange as the disk impinges on the baffle is

(25)

$$(P_o)_s = \frac{\rho_o V_{4'}^2}{g_o}$$

$$= \frac{0.394(3800)^2}{32.2(144)} = 1227 \text{ PSI}$$

The total pressure felt at the extremity of the baffle is therefore

(26) $P_{o\ \text{total}} = 1227 + 283 = 1510$ psi

Using a similar procedure the distribution of total pressure can be mapped for the entire baffle. The following sections will describe the results of calculations for the pressure distribution throughout the brake interior.

INITIAL PRESSURE DISTRIBUTION IN THE 4" LONG DIFFUSER SECTION

The pressure distribution imposed radially upon the diverging diffuser section by the isentropic gas expansion directly behind the base of the projectile is computed from (11) and summarized in the following table.

Table 1

Diffuser Diameter (in)	Radial Pressure (Psi)
5	5724
6	3629
7	2468

Following the "uncorking" of the diffuser by the projectile base, the diffuser pressures will decrease rapidly tending toward the steady values. As a consequence the values given in Table 1 should represent the maximum pressures experienced by the diffuser.

INITIAL PRESSURE DISTRIBUTION ON THE SIDE PLATES BETWEEN THE DIFFUSER AND BAFFLE

Following the uncorking of the diffuser the results of a one-dimensional shock expansion from the "windows" of the brake yield the following initial side plate pressure distributions:

Table 2
(1" from Diffuser Exit)

Distance from Center Line (in)	Pressure (Psi)
0 - 2.83"	2468
3.0	1864
3.5	759
4.0	284
4.5	95
5.0	28

Table 3
(2" from Diffuser Exit)

Distance from Center Line (in)	Pressure (Psi)
0 - 2.17	2468
2.5	1860
3.0	1202
3.5	759
4.0	470
4.5	285
5.0	167

Table 4
(3" from Diffuser Exit)

Distance from Center Line (in)	Pressure (Psi)
0 - 1.5	2468
2.0	1860
2.5	1391
3.0	1035
3.5	759
4.0	552
4.5	399
5.0	283

The location of the pressure stations cited in Tables 2-4 are shown in Figure 5.

INITIAL PRESSURE DISTRIBUTION ON THE BAFFLE

The total pressures which are imposed initially by the arrival of the gases directly behind the projectile base are shown in Table 5. The location of the pressure stations used are shown in Figure 6. These are calculated by the method shown previously using equations (22) through (26).

Table 5

Distance from Center Plane (in)	Pressure (Psi)
0 - 1.5	9413
2.0	7397
2.5	5782
3.0	4501
3.5	3462
4.0	2648
4.5	2015
5.0	1510

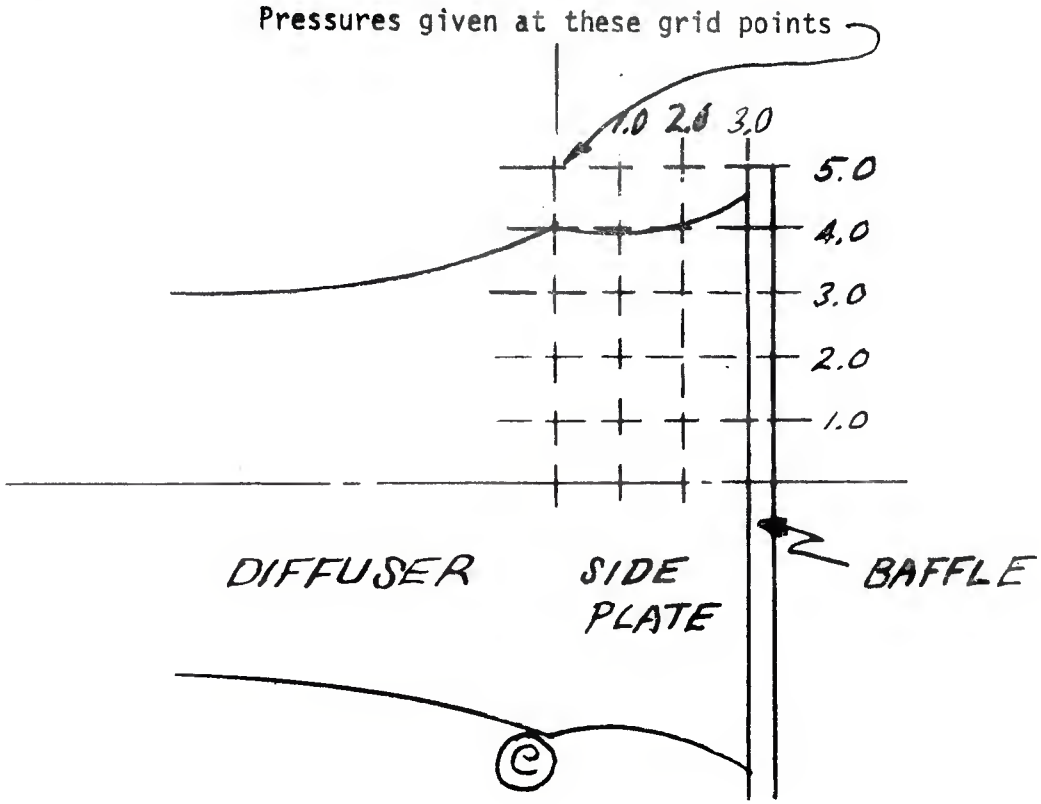

Figure 5. Location of side plate pressure stations.

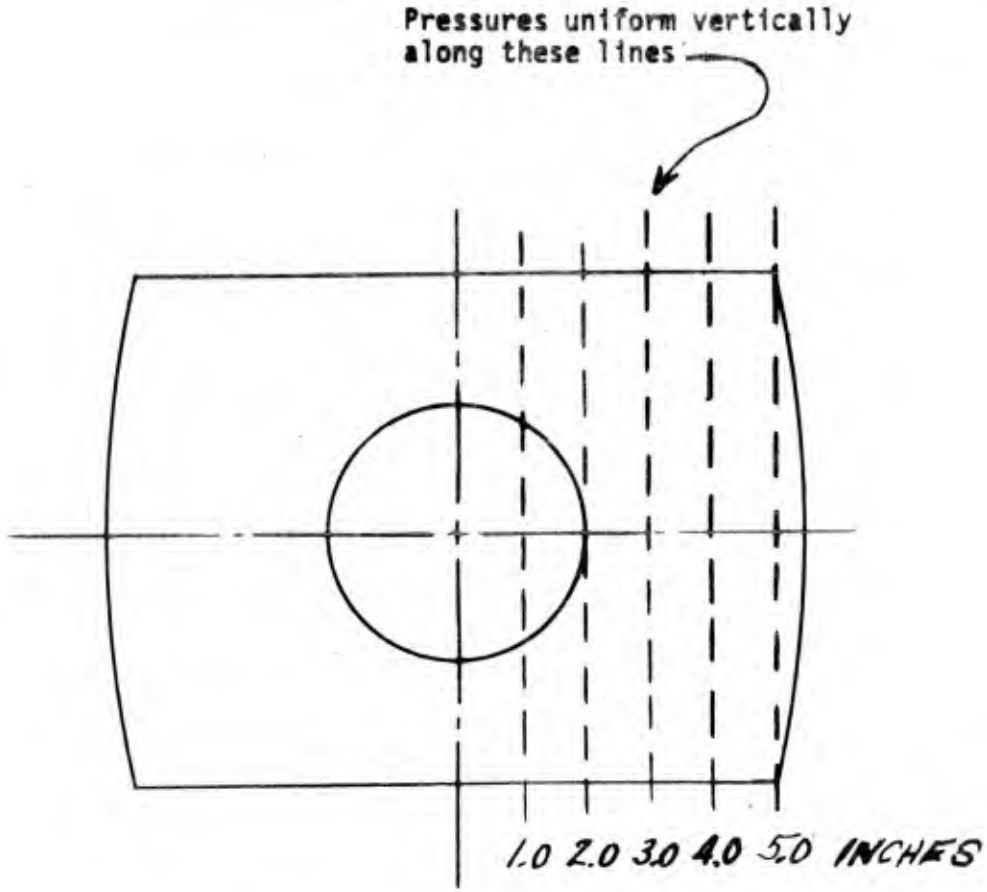

Figure 6. Location of baffle pressure stations.

These values are the stagnation pressures obtained by summing both the static and dynamic pressures.

All interior surfaces of the brake will experience some pressures prior to those listed above due to the precursor flow caused by blow-by. These pressures are expected, however, to be masked in time and amplitude by the almost simultaneous arrival of the uncorking flows.

SECOND STAGE ANALYSIS

The techniques described above can be extended to the analysis of a second stage of the muzzle brake with some slight modifications.

Figure 7 shows the wave diagram for the radial motion of gas in the second stage as the disk of gas expands behind the projectile base. The only backward running characteristics generated in the first stage which pass into the second stage are those directly behind the projectile base when it passes through the first baffle. If it is assumed that this baffle is quite thin, then the burst of gases into the second stage gives rise to a new centered expansion fan as shown in Figure 7.

From the previous calculations of the values in Table 4, the conditions two inches from the center line at the moment that the projectile passes through the first baffle are

$$C_{4''} = 2463 \text{ ft/sec}$$

$$T_{4''} = 2250 \text{ °R}$$

$$\rho_{4''} = 1.778 \text{ lbm/ft}^3 \tag{27}$$

$$P_{4''} = 1860 \text{ psia}$$

$$U_{4''} = 563.6 \text{ ft/sec}$$

The shock Mach number for the radial growth of the disk after it passes through the first baffle plate is given by (28) which is similar

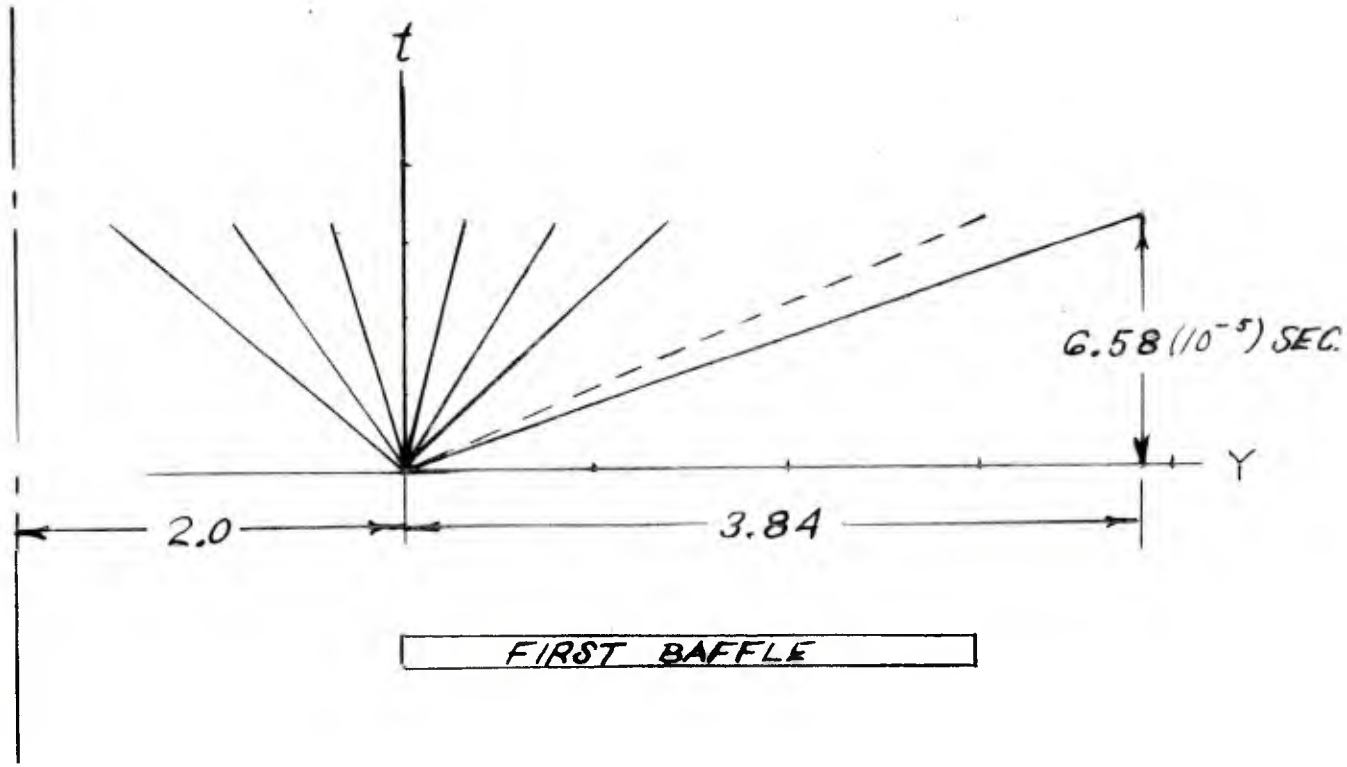

Figure 7. Wave diagram for second baffle.

to (3) and (15).

(28)
$$\frac{P_4''}{P_1} = \frac{\left[\frac{2\gamma_1 M_s^2 - (\gamma_1 - 1)}{\gamma_1 + 1}\right]}{\left[1 - \left(\frac{\gamma_4 - 1}{\gamma_1 + 1}\right)\frac{C_1}{C_4}\left(M_s - \frac{1}{M_s}\right) + \left(\frac{\gamma_4 - 1}{2}\right)\frac{U_4''}{C_4''}\right]^{\frac{2\gamma_4}{\gamma_4 - 1}}}$$

$$124 = \frac{1.167 M_s^2 - 0.286}{\left[1.0286 - 0.0478\left(M_s - \frac{1}{M_s}\right)\right]^{10}}$$

The shock Mach number which satisfies this equation is $M_s = 4.3$. The velocity of the gas behind this shock wave is from (4)

(4)
$$U_2'' = \frac{2}{\gamma_1 + 1} C_1 \left(M_s - \frac{1}{M_s}\right)$$

$$= \frac{2}{2.4} (1130) \left(4.3 - \frac{1}{4.3}\right)$$

$$U_2'' = 3830 \text{ ft/sec}$$

The pressure in this region is from (6).

(29)
$$\frac{P_2''}{P_1} = \frac{2\gamma_1}{\gamma_1 + 1} M_s^2 - \left(\frac{\gamma_1 - 1}{\gamma_1 + 1}\right) = 21.4$$

$$P_2'' = 321 \text{ psi}$$

If the distance between the first and second baffles is assumed to be 3.0 inches, then the shock wave will have advanced radially a distance equal to

(30)
$$3\left(\frac{M_s C_1}{3800}\right) = 3\left(\frac{1130(4.3)}{3800}\right) = 3.84"$$

which is 0.84" beyond the edge of the second baffle at this point, assuming that the second baffle is the same size as the first baffle.

The characteristic which forms the left side of the expansion fan coincides with characteristic along which U_4'' and C_4'' have constant values of

$$U_{4"} = 563.6 \text{ ft/sec}$$

$$C_{4"} = 2463 \text{ ft/sec}$$

from (27).

Regions 4" and 3" are connected by a forward running characteristic along which

(31) $$U_{4"} = \frac{2}{\gamma_4 - 1} C_{4"} = U_{3"} + \frac{2}{\gamma_4 - 1} C_{3"}$$

$$563.6 + 8(2463) = 3830 + 8C_{3"}$$

$$C_{3"} = 2055 \text{ ft/sec}$$

Then from (13)

(32) $$T_{3"} = T_{4"}\left(\frac{C_{3"}}{C_{4"}}\right)^2$$

$$T_{3"} = 2250 \left(\frac{2055}{2463}\right)^2$$

$$T_{3"} = 1566 \text{ °R}$$

from (12)

(33) $$P_{3"} \quad P_{4"} \left(\frac{T_{3"}}{T_{4"}}\right)^{\frac{\gamma_4}{\gamma_4 - 1}}$$

$$P_{3"} = 304 \text{ psia}$$

(34) from (8) $$\rho_{3"} = \rho_{4"} \quad \frac{P_{3"}}{P_{4"}} \quad \frac{T_{4"}}{T_{3"}}$$

$$= 1.778 \frac{304}{1860} \quad \frac{2250}{1566}$$

$$\rho_{3"} = 0.132$$

and from (25) the stagnation pressure is

(35) $$(P_{3"})_s = \frac{\rho_3 V^2}{g_o}$$

$$= \frac{0.132}{32.2} \left(\frac{3800}{12}\right)^2$$

$$P_{3"_s} = 411 \text{ psi}$$

The total pressure in the constant velocity region behind the shock wave is therefore

(36) $$304 + 411 = 715 \text{ psia}$$

The leading edge of the expansion fan has a slope

(37) $$U_{3"} - C_{3"} = U_{2"} - C_{3"}$$
$$= 3830 - 2055$$
$$= 1775 \text{ ft/sec}$$

The radial position of the leading edge of the fan at the second baffle is

(38) $$\triangle R^1 = (1775)6.58(10^{-5})(12) = 1.40 \text{ in}$$

Referring to Figure 7 and (36) shows that the outer 1.6 inches of the second baffle plate has a constant total pressure of 715 psia impressed upon it.

The backward running characteristic coincident with the hole in the second baffle has a zero slope on the wave diagram so that $U_i - C_i = 0$ or $U_i = C_i$ along this characteristic. The forward running characteristic which connects the hole with the backward running characteristic at the edge of the fan carries a constant value of $U + \frac{2}{\gamma_4 - 1} C$ so that

(39) $$U_i + \left(\frac{2}{\gamma_4 - 1}\right) C_i = U_{4"} + \left(\frac{2}{\gamma_4 - 1}\right) C_{4"} \text{ or}$$
$$U_i + \left(\frac{2}{\gamma_4 - 1}\right) C_i = 563.6 + 8\ (2463)$$

where U_i and C_i are the velocity and sound speed at the edge of the hole. Therefore

$$9U_i = 9C_i = 563.6 + 8(2463)$$
$$U_i = C_i = 2252 \text{ ft/sec}$$

Then as previously

(40) $$T_i = T_{4"} \left(\frac{Ci}{C_{4"}}\right)^2$$

$$= 2250 \left(\frac{2252}{2463}\right)^2$$

$$T_i = 1881 \ ^\circ R$$

(41) $$P_i = P_{4"} \left(\frac{T_i}{T_{4"}}\right)^5$$

$$= 1860 \left(\frac{1881}{2250}\right)^5$$

$$P_i = 760 \text{ psia}$$

(42) $$\rho_i = \rho_{4"} \left(\frac{Pi}{P_{4"}}\right)^{\frac{1}{\gamma_4}}$$

$$= 1.778 \left(\frac{(760)}{1860}\right)^{.8}$$

$$\rho_i = 0.869 \text{ lbm/ft}^3$$

The stagnation pressure at the hole's edge is then

(43) $$(P_i)_s = \frac{\rho_i \ V^2}{go}$$

$$= \frac{0.869}{32.2} \left(\frac{3800}{12}\right)^2$$

$$(P_i)_s = 2706 \text{ psi}$$

The total pressure at the hole of the second baffle 2.0 inches from the center plane is 2706 + 760 = 3466 psia.

The pressure distribution throughout the fan can be computed in the same manner as for the first baffle. Comparing the pressures on the second baffle with those on the first (see Table 5) shows that the stagnation pressures on the second baffle at the hole and outside edge

are roughly one-half those experienced by the first baffle plate. The total force on the second baffle plate would, however, be somewhat less than one-half the force on the first baffle due to the fact that a large portion of the second baffle's area is exposed to a constant pressure of 715 psia.

The pressures on the side plates of the second stage are considerably lower than those on the first stage, ranging from 760 along the center plane to 304 just behind the shock wave.

Portions of the side plate behind the first baffle will be beyond the leading edge of the shock wave in the additional 66 microseconds covered by this analysis. Pressurization of these areas at future times will result from the complex flows which are established following the collision of the leading gas disk with the baffle.

ESTABLISHMENT OF STEADY FLOW

The condition of steady state flow will be attained when roughly the backward running characteristic (which is actually swept downstream in this case) reaches the end of the diffuser. The time at which this occurs can be estimated by examining

(44) $$U_4 - C_4 = 3800-2918 = 882$$

which is roughly the speed with which pressure signals are swept downstream through the diffuser. Steady flow is attained in the time interval

(45) $$\triangle t = \frac{4"/12}{882} = 33.3(10^{-5}) \text{ sec}$$

The projectile leaves the second stage baffle at

(46) $$t = \frac{10/12}{3800} = 22\ (10^{-5}) \text{ sec}$$

so that very shortly after the projectile clears the muzzle brake the diffuser flow becomes steady (assuming the muzzle conditions are quasi-steady).

Steady flow calculations through an area ratio 49/16, i.e., from the entrance to exit of the diffuser section show that the steady state exit conditions are as listed in Table 6 along with those for Region 4' immediately behind the projectile as it uncorks the diffuser. These latter are given by equations (11) through (13).

Table 6

	Steady State	Behind Projectile Base
T_e	2068 °R	2381 °R
C_e	2364 fps	2534 fps
V_e	6146 fps	3800 fps
P_e	1220 psia	2468 psia

The major changes which occur during the transition period to steady state occur in the exit velocity V_e and the exit pressure. As far as the side plates are concerned, this change is advantageous. Due to the increase in exit velocity, it is difficult to say whether the steady state is better or worse than the transient effects analyzed above.

EXTERNAL DISTRIBUTION LIST

May 1976

1 copy to each

CDR
US ARMY MAT & DEV READ. COMD
ATTN: DRCRD
DRCRD-TC
DRCRD-W
5001 EISENHOWER AVE
ALEXANDRIA, VA 22304

OFC OF THE DIR. OF DEFENSE R&E
ATTN: ASST DIRECTOR MATERIALS
THE PENTAGON
WASHINGTON, D.C. 20315

CDR
US ARMY TANK-AUTMV COMD
ATTN: AMDTA-UL
AMSTA-RKM MAT LAB
WARREN, MICHIGAN 48090

CDR
PICATINNY ARSENAL
ATTN: SARPA-TS-S
SARPA-VP3 (PLASTICS
TECH EVAL CEN)
DOVER, NJ 07801

CDR
FRANKFORD ARSENAL
ATTN: SARFA
PHILADELPHIA, PA 19137

DIRECTOR
US ARMY BALLISTIC RSCH LABS
ATTN: AMXBR-LB
ABERDEEN PROVING GROUND
MARYLAND 21005

CDR
US ARMY RSCH OFC (DURHAM)
BOX CM, DUKE STATION
ATTN: RDRD-IPL
DURHAM, NC 27706

CDR
WEST POINT MIL ACADEMY
ATTN: CHMN, MECH ENGR DEPT
WEST POINT, NY 10996

CDR
US ARMY ARMT COMD
ATTN: AMSAR-PPW-IR
AMSAR-RD
AMSAR-RDG
ROCK ISLAND, IL 61201

CDR
US ARMY ARMT COMD
FLD SVC DIV
ARMCOM ARMT SYS OFC
ATTN: AMSAR-ASF
ROCK ISLAND, IL 61201

CDR
US ARMY ELCT COMD
FT MONMOUTH, NJ 07703

CDR
REDSTONE ARSENAL
ATTN: AMSMI-RRS
AMSMI-RSM
ALABAMA 35809

CDR
ROCK ISLAND ARSENAL
ATTN: SARRI-RDD
ROCK ISLAND, IL 61202

CDR
US ARMY FGN SCIENCE & TECH CEN
ATTN: AMXST-SD
220 7TH STREET N.E.
CHARLOTTESVILLE, VA 22901

DIRECTOR
US ARMY PDN EQ. AGENCY
ATTN: AMXPE-MT
ROCK ISLAND, IL 61201

CDR
HQ, US ARMY AVN SCH
ATTN: OFC OF THE LIBRARIAN
FT RUCKER, ALABAMA 36362

EXTERNAL DISTRIBUTION LIST (Cont)

1 copy to each

CDR
US NAVAL WPNS LAB
CHIEF, MAT SCIENCE DIV
ATTN: MR. D. MALYEVAC
DAHLGREN, VA 22448

DIRECTOR
NAVAL RSCH LAB
ATTN: DIR. MECH DIV
WASHINGTON, D.C. 20375

DIRECTOR
NAVAL RSCH LAB
CODE 26-27 (DOCU LIB.)
WASHINGTON, D.C. 20375

NASA SCIENTIFIC & TECH INFO FAC
PO BOX 8757, ATTN: ACQ BR
BALTIMORE/WASHINGTON INTL AIRPORT
MARYLAND 21240

DEFENSE METALS INFO CEN
BATTELLE INSTITUTE
505 KING AVE
COLUMBUS, OHIO 43201

MANUEL E. PRADO / G. STISSER
LAWRENCE LIVERMORE LAB
PO BOX 808
LIVERMORE, CA 94550

DR. ROBERT QUATTRONE
CHIEF, MAT BR
US ARMY R&S GROUP, EUR
BOX 65, FPO N.Y. 09510

2 copies to each

CDR
US ARMY MOB EQUIP RSCH & DEV COMD
ATTN: TECH DOCU CEN
FT BELVOIR, VA 22060

CDR
US ARMY MAT RSCH AGCY
ATTN: AMXMR - TECH INFO CEN
WATERTOWN, MASS 02172

CDR
WRIGHT-PATTERSON AFB
ATTN: AFML/MXA
OHIO 45433

CDR
REDSTONE ARSENAL
ATTN: DOCU & TECH INFO BR
ALABAMA 35809

12 copies

CDR
DEFENSE DOCU CEN
ATTN: DDC-TCA
CAMERON STATION
ALEXANDRIA, VA 22314

NOTE: PLEASE NOTIFY CDR, WATERVLIET ARSENAL, ATTN: SARWV-RT-TP, WATERVLIET, N.Y. 12189, IF ANY CHANGE IS REQUIRED TO THE ABOVE.

WATERVLIET ARSENAL INTERNAL DISTRIBUTION LIST

May 1976

	No. of Copies
COMMANDER	1
DIRECTOR, BENET WEAPONS LABORATORY	1
DIRECTOR, DEVELOPMENT ENGINEERING DIRECTORATE	1
ATTN: RD-AT	1
RD-MR	1
RD-PE	1
RD-RM	1
RD-SE	1
RD-SP	1
DIRECTOR, ENGINEERING SUPPORT DIRECTORATE	1
DIRECTOR, RESEARCH DIRECTORATE	2
ATTN: RR-AM	1
RR-C	1
RR-ME	1
RR-PS	1
TECHNICAL LIBRARY	5
TECHNICAL PUBLICATIONS & EDITING BRANCH	2
DIRECTOR, OPERATIONS DIRECTORATE	1
DIRECTOR, PROCUREMENT DIRECTORATE	1
DIRECTOR, PRODUCT ASSURANCE DIRECTORATE	1
PATENT ADVISORS	1